electrode at slow scan rates may be attributed to this reaction. At slow scan rates more time is available for the cross reaction (5) to occur.

The above electrochemical study leads to the conclusion that the reduction of Cu_2L produces kinetically labile species. Unfortunately, the $[Cu_2L]^-$ and $[Cu_2L]^{2-}$ species appear to be too reactive to isolate and characterize by controlled-potential electrolysis, as decomposition occurs in the longer time scale experiments. The difference in $E_{1/2}(1)$ and $E_{1/2}(2)$ is clearly less than that for **10**.[27] However, the half-reduced form of this compound is relatively stable and shows an ESR signal for the mixed-valence species consistent with the electron being delocalized between the metal ions at ambient temperature but localized on one metal ion at 77 K.[27] The localized/delocalized electron configuration could conceivably be important in this work as indicated in the electrochemical data and may represent the α and β forms of the Cu_2L^- complexes.

Long and Hendrickson[34] found that while some of this class of compounds gave a seven-line ESR signal at ambient temperature, others gave a four-line signal consistent with a localized electron. In addition, the differential pulse voltammogram of one of the binuclear copper(II) compounds showed a reduction process intermediate to the two main processes.[34] This compound was among those showing electron localization at ambient temperature. Similarly Drago et al.[35] examined the electrochemistry of a binuclear complex related to **2** but with an ethoxide exogenous bridge (X). When it was electrolyzed to the half-reduced state, a four-line ESR signal was observed at ambient temperature as in the frozen state. These observations coupled with our work are consistent with the existence of processes of dynamic isomerization with rate and equilibrium constants of significant variability highly dependent on the ligand structure.

X-ray photoelectron spectroscopy by Gagne et al.[51] and finally a crystal structure determination[44] have revealed the presence of the genuine mixed-oxidation-state center $Cu^+ \cdot Cu^{2+}$, in the solid state, rather than a delocalized structure for compound **10**. The mechanism for electron delocalization is probably through dynamic isomerization as described in this work. The contribution from the magnetic exchange coupling was evaluated to be 6 mV[31] for the singlet–triplet energy separation ($2J$) of -586 cm^{-1}. This magnitude in potential is consistent with the electrochemical behavior described above. It has also been recently observed that minor conformational changes associated with related binuclear copper(II) complexes do occur and give rise to significant differences in exchange coupling[52] and consequently a small change in the reduction potential. Thus, the structural change proposed in this work may be associated with isomerization, resulting in a spin change of the kind described above. In conclusion, the present work demonstrates that a much closer examination of the electrochemical data is required to determine whether models based on simple electron charge-transfer steps are appropriate. In the present example this is clearly not the case. Further studies are required to ascertain whether other binuclear complexes exhibit similar electrochemical behavior. Clearly, the flexibility of the binuclear complex is important in determining the reversibility or otherwise of the reduction processes as are other structural features.[25-39,53-55]

Although the redox processes reported here occur at potentials that are more negative than those in the type 3 sites in copper proteins, the model compound **6**, like many other similar phenoxide-bridged copper(II) complexes, is capable of acting as a two-electron center. Consequently, these model compounds contribute to the better understanding of the possible stereochemical interactions of the type 3 copper compounds associated with electron transfer.

Acknowledgment. We thank the Australian Research Grants Scheme and the Monash University Special Research Grants (K.S.M.) for financial support. W.M. thanks the Public Service Board of Australia for a Postgraduate Scholarship. Kevin Berry is thanked for experimental assistance.

Registry No. **5**, 96705-28-1; **6**, 96689-03-1; **11**, 6327-85-1; **12**, 34920-23-5; **13**, 96689-00-8; **14**, 96689-01-9; $[Cu_2L]^-$, 96689-04-2; $[Cu_2L]^{2-}$, 96689-05-3; 2,6-bis(hydroxymethyl)-4-methylphenol, 91-04-3; 2,6-bis((salicylideneamino)methyl)-4-methylphenol, 96689-02-0.

(51) Gagne, R. R.; Allison, J. L.; Koval, C. A.; Mialki, W. S.; Smith, T. J.; Walton, R. A. *J. Am. Chem. Soc.* **1980**, *102*, 1905.
(52) Fallon, G. D.; Murray, K. S.; Mazurek, W.; O'Connor, M. J. *Inorg. Chim. Acta* **1985**, *96*, L53.
(53) Coughlin, P. K.; Lippard, S. J. *Inorg. Chem.* **1984**, *23*, 1446.
(54) Doine, H.; Stephens, F. F.; Cannon, R. D. *Inorg. Chim. Acta* **1983**, *75*, 155.
(55) Mohapatra, B. K.; Sahoo, B. *Indian J. Chem. Sect. A* **1983**, *22A*, 494.
(56) Nicholson, R. J. *Anal. Chem.* **1966**, *38*, 1406.

Contribution from the Department of Chemistry, Purdue University, West Lafayette, Indiana 47907

Stability Constant and Reaction Mechanisms of the Nickel(II)–Tripeptide Complex of α-Aminoisobutyric Acid

WILLIAM R. KENNEDY and DALE W. MARGERUM*

Received March 4, 1985

The $Ni^{II}(H_{-2}Aib_3)^-$ complex (Aib is the α-aminoisobutyryl residue) is unusually stable and is relatively sluggish in its reactions with acid and with cyanide ion. The β_{1-21} stability constant (for Ni^{2+} and $L^- \rightleftarrows Ni(H_{-2}L)^- + 2H^+$) is $10^{-9.65}$ M, which is 1500 times larger for L = Aib_3 than for L = G_3 (G is the glycyl residue). The rate of acid dissociation for $Ni^{II}(H_{-2}Aib_3)^-$ is 3400–390000 times slower than for the G_3 complex. Cyanide ion reacts rapidly to form $Ni^{II}(H_{-2}Aib_3)(CN)^{2-}$, which then has a $[CN^-]^2$ dependence to give $Ni(CN)_4^{2-}$. The third-order rate constant is 13 M^{-2} s^{-1}, which is 100 times smaller than for the corresponding reactions with the G_3 complex. The stability and kinetic effects of $Ni^{II}(H_{-2}Aib_3)^-$ are attributed, in large part, to the increase in the nickel–N(peptide) bond strength due to the α-carbon methyl groups.

Introduction

The α-aminoisobutyryl (Aib) residue is present in peptides that act as microbial antibiotics.[1-3] The presence of adjacent Aib residues in peptides restricts their conformation, due to steric effects of the two methyl groups on the α-carbons.[4,5] The absence of hydrogens on the α-carbons is important in the stabilization of Aib_3 complexes of copper(III) and nickel(III).[6] These tripeptide complexes are relatively slow to undergo self-redox decomposition.[6]

(1) Mueller, P.; Rudin, D. O. *Nature (London)* **1968**, *217*, 713.
(2) Martin, D. R.; Williams, R. J. P. *Biochem. J.* **1976**, *153*, 181.
(3) Jung, G.; Konig, W. A.; Liebfritz, D.; Ooka, T.; Janko, K.; Boheim, G. *Biochim. Biophys. Acta* **1976**, *433*, 164.
(4) Nagaraj, R.; Shamala, N.; Balaram, P. *J. Am. Chem. Soc.* **1979**, *101*, 16.
(5) Rao, C. P.; Nagaraj, R.; Rao, C. N. R.; Balaram, P. *Biochemistry* **1980**, *19*, 423.

0020-1669/85/1324-2490$01.50/0

This has permitted X-ray crystal structure determination of the copper(III)–Aib_3 complex[7] and measurement of the self-exchange rate constants for the Cu(III)–Cu(II) complexes by proton NMR line broadening.[8] The relative effect of the inductive and steric properties of the α-carbon methyl groups on the ability of peptides to bind to copper(II) was examined recently.[9] Various other studies have been performed on the Aib_3 complexes of copper(III)[10-12] and nickel(III).[13-16]

The $Ni^{II}(H_{-2}Aib_3)^-$ complex (structure I) is a yellow, diamagnetic species. A crystal structure determination[17] shows that it is essentially square planar, with strong bonds between the two

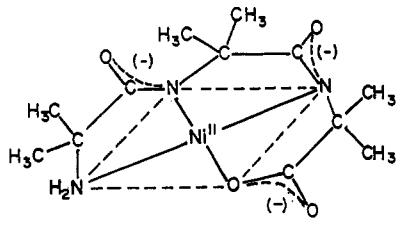

I

deprotonated peptide nitrogen atoms and nickel. EXAFS analysis of the complex in frozen aqueous solution also gives a coordination number of four and the same average bond distances.[17] In general, nickel(II)–peptide complexes are readily formed by addition of base to a solution of the metal ion and peptide ligand. For many peptides, equilibrium is established in a few seconds or minutes after each addition. However, when Aib_3 is the ligand, the pH must be raised slowly, over a period of many hours, to prevent the precipitation of nickel hydroxide. Once the hydroxide forms, the mixtures are exceedingly slow to adjust to equilibrium conditions. Initially, it was not clear if this behavior was due to a weak nickel(II)–Aib_3 complex that could not compete with $Ni(OH)_2$ or if the behavior was due to sluggish rates of formation of the complex. Tests of the rates of acid decomposition of the $Ni^{II}(H_{-2}Aib_3)^-$ complex, once it was formed, showed these reactions to be many orders of magnitude slower than those of $Ni^{II}(H_{-2}G_3)^-$. This is in marked contrast to the behavior of $Cu^{II}(H_{-2}Aib_3)^-$ as compared to that of $Cu^{II}(H_{-2}G_3)^-$, where the proton rate constants are of the same order of magnitude.[18,19]

In the present work the stability constant of the $Ni^{II}(H_{-2}Aib_3)^-$ complex (eq 1) is determined. This cannot be done by potentiometric titration, a method of choice for similar complexes,[9,20,21] because the excessive time required for the titration introduces sources of error that invalidate the procedure. Instead, we use acid equilibration studies, over the period of 16–26 days, to measure the stability constant, β_{1-21} (the subscripts refer to the number of metal ions, protons, and ligands, respectively, in the complex). We find that β_{1-21} is much larger for Aib_3 than for G_3.

$$Ni^{2+} + Aib_3^- \overset{\beta_{1-21}}{\rightleftharpoons} Ni^{II}(H_{-2}Aib_3)^- + 2H^+ \qquad (1)$$

The kinetics of acid dissociation are measured from pH 0.5 to 7.5, and a mechanism is proposed for this process. We also report the kinetics of the cyanide ion reactions to displace Aib_3 from the nickel and form $Ni(CN)_4^{2-}$. Initially, it was our intention to determine the β_{1-21} constant by competitive reactions with cyanide ion. However, a mixed complex, $Ni^{II}(H_{-2}Aib_3)(CN)^{2-}$, forms and interferes with the measurements. Also, the equilibration reactions are sufficiently slow that peptide hydrolysis becomes a serious problem in base. Mechanisms are proposed for the cyanide ion displacement reactions.

Table I. Observed Protonation Rate Constants for the Reaction of $Ni^{II}(H_{-2}Aib_3)^-$ with Acid[a]

−log [H+]	buffer[b]	k°_{obsd},[c] s^{-1}	−log [H+]	buffer[b]	k°_{obsd},[c] s^{-1}
0.30	N	1.42	4.39	A	1.34×10^{-3}
0.52	N	0.882	4.59	A	8.90×10^{-4}
1.00	N	0.416	4.79	A	5.30×10^{-4}
1.30	N	0.311	4.89	A	2.80×10^{-4}
1.60	N	0.217	5.29	A	7.77×10^{-5}
1.89	C	0.158	5.49	A	6.42×10^{-5}
2.09	C	0.121	5.69	A	4.39×10^{-5}
2.29	C	8.30×10^{-2}	6.73	P	1.3×10^{-5}
2.49	C	5.76×10^{-2}	6.83	P	6.4×10^{-6}
2.69	C	4.54×10^{-2}	6.95	P	6.1×10^{-6}
2.89	C	3.12×10^{-2}	7.04	P	3.2×10^{-6}
3.09	C	2.05×10^{-2}	7.15	P	2.5×10^{-6}
3.29	C	1.25×10^{-2}	7.24	P	1.4×10^{-6}
3.49	A	9.80×10^{-3}	7.31	P	1.6×10^{-6}
3.69	A	7.01×10^{-3}	7.5	P	8.9×10^{-7}
3.89	A	4.54×10^{-3}	7.6	P	3.5×10^{-7}
4.09	A	2.34×10^{-3}	7.6	P	3.1×10^{-7}
4.29	A	1.65×10^{-3}	7.7	P	3.5×10^{-7}

[a] $[Ni^{II}(H_{-2}Aib_3)]_{tot} = 2.5 \times 10^{-4}$ M, μ = 1.0 ($NaClO_4$), 25.0 (1) °C, 415 or 250 nm; all k°_{obsd} values reported are extrapolated to zero buffer concentration, except as noted below. [b] Key: N, no buffer; C, chloroacetic acid (0.015–0.03 M); A, acetic acid (0.015–0.03 M); P, phosphate (0.002 M), estimated from initial rates of equilibrium reactions, no buffer effect subtracted. [c] $k^\circ_{obsd} = k_{obsd} - k_{HB}[HB]$.

Experimental Section

Nickel(II) perchlorate, prepared from $NiCO_3$ and $HClO_4$, was standardized by EDTA titration with murexide indicator. The tripeptide, α-aminoisobutyryl-α-aminoisobutyryl-α-aminoisobutyric acid (Aib_3), was prepared by Lee or Hamburg as previously reported.[6] The $Ni^{II}(H_{-2}Aib_3)^-$ solutions were freshly prepared for each set of experiments by mixing the tripeptide with a solution of nickel(II) in a 1.1:1.0 mole ratio. This solution was raised to pH 10.0 over the period of 3–8 h by the addition of NaOH. Ionic strength was maintained at 0.1 or 1.0 M with $NaClO_4$. Buffers were prepared from glacial acetic acid or chloroacetic acid. These stock solutions were standardized with base and phenolphthalein indicator. Borate buffers were made from $Na_2B_4O_7 \cdot 10H_2O$. Cyanide solutions were freshly prepared for each set of experiments with NaCN. Stock solutions were standardized by argentometry in the presence of iodide. All pH measurements were performed on an Orion 601A pH meter using an Orion combination pH electrode, which was calibrated to yield the relationships −log [H+] = pH + 0.29 at μ = 1.0 M ($NaClO_4$) and 25.0 ± 0.1 °C and −log [H+] = 1.0139pH + 0.06 at μ = 0.1 M ($NaClO_4$) and 25.0 ± 0.1 °C.

Acid dissociation kinetics and equilibrium reactions were monitored by the loss of absorbance of the nickel complex at either 415 nm (ϵ = 250 M^{-1} cm^{-1}) or 250 nm (ϵ = 6260 M^{-1} cm^{-1}) on a Durrum-Gibson stopped-flow spectrophotometer interfaced to an HP 2100 minicomputer, a Perkin-Elmer 320 spectrophotometer interfaced to a PE 3600 Data Station, a Cary 16 spectrophotometer interfaced to an Intel 8008 microprocessor, or a Cary 14 spectrophotometer. All reactions were well buffered and were run at 25.0 ± 0.1 °C. Excellent first-order kinetics were observed, with the pseudo-first-order rate constant defined by eq 2 and 3. Pseudo-first-order rate constants were obtained from the slope

$$-d[Ni^{II}(H_{-2}Aib_3)]_{tot}/dt = k_{obsd}[Ni^{II}(H_{-2}Aib_3)]_{tot} \qquad (2)$$

$$[Ni^{II}(H_{-2}Aib_3)]_{tot} = [Ni^{II}(H_{-2}Aib_3)^-] + [Ni^{II}(H_{-2}Aib_3)H] \qquad (3)$$

of a plot of ln $(A - A_\infty)$ vs. time, taken over 3–4 half-lives of the reaction. The reported rate constants are either the average of three runs at the same conditions or the result of extrapolation to zero buffer concentration

(6) Kirksey, S. T., Jr.; Neubecker, T. A.; Margerum, D. W. *J. Am. Chem. Soc.* **1979**, *101*, 1631.
(7) Diaddario, L. L.; Robinson, W. R.; Margerum, D. W. *Inorg. Chem.* **1983**, *22*, 1021.
(8) Koval, C. A.; Margerum, D. W. *Inorg. Chem.* **1981**, *20*, 2311.
(9) Hamburg, A. W.; Nemeth, M. T.; Margerum, D. W. *Inorg. Chem.* **1983**, *22*, 3535.
(10) Hamburg, A. W.; Margerum, D. W. *Inorg. Chem.* **1983**, *22*, 3884.
(11) Raycheba, J. M. T.; Margerum, D. W. *Inorg. Chem.* **1981**, *20*, 45.
(12) Youngblood, M. P.; Margerum, D. W. *Inorg. Chem.* **1980**, *19*, 3068.
(13) Raycheba, J. M. T.; Margerum, D. W. *Inorg. Chem.* **1981**, *20*, 1441.
(14) Murray, C. K.; Margerum, D. W. *Inorg. Chem.* **1982**, *21*, 3501.
(15) Murray, C. K.; Margerum, D. W. *Inorg. Chem.* **1983**, *22*, 463.
(16) Owens, G. D.; Phillips, D. A.; Czarnecki, J. J.; Raycheba, J. M. T.; Margerum, D. W. *Inorg. Chem.* **1984**, *23*, 1345.
(17) Kennedy, W. R.; Powell, D.; Niederhoffer, E. C.; Teo, B.-K.; Orme-Johnson, W. H.; Margerum, D. W., to be submitted for publication.
(18) Dickson, P. N.; Margerum, D. W., unpublished results.
(19) Pagenkopf, G. K.; Margerum, D. W. *J. Am. Chem. Soc.* **1968**, *90*, 6963.
(20) Kim, M. K.; Martell, A. E. *J. Am. Chem. Soc.* **1967**, *89*, 5138.
(21) Kim, M. K.; Martell, A. E. *J. Am. Chem. Soc.* **1969**, *91*, 872.

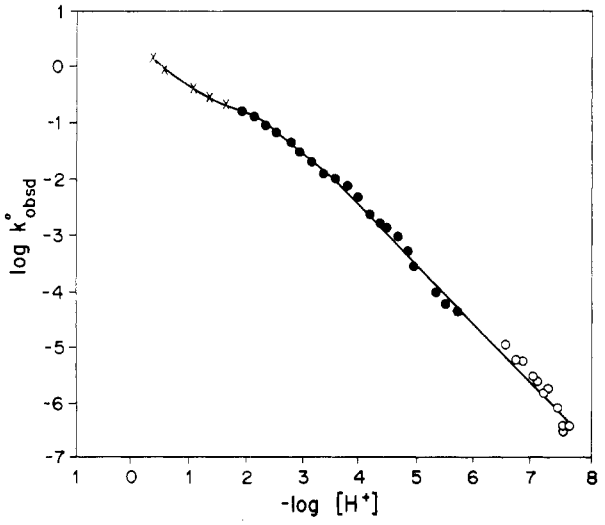

Figure 1. Dependence of the dissociation rate constant of $Ni^{II}(H_{-2}Aib_3)^-$ on acidity. The solid line is calculated by using eq 10 with the values of the constants listed in Table II. ×, points for reaction with no buffer; ●, points for buffered reaction, with buffer contribution subtracted; ○, points from initial rates of equilibrium reactions, with no buffer effect subtracted.

of three runs at different buffer concentrations. The observed rate constants typically have a standard deviation of 1–3%.

One set of experiments was performed on a vidicon–stopped-flow spectrophotometer,[22] which permited the acquisition of a series of 50 spectra in a few hundred milliseconds.

Observed dissociation rate constants are also reported for the reactions that were used for the equilibrium studies. These were obtained by the method of initial rates, over the first half-life of the reaction.

Cyanide reactions were monitored by the absorbance of $Ni(CN)_4^{2-}$ at 285 nm on the stopped-flow or other spectrophotometers. The overall reaction is defined by eq 4. Under the conditions investigated, Ni-

$$Ni^{II}(H_{-2}Aib_3)^- + 4CN^- + 2H_2O \rightarrow Ni(CN)_4^{2-} + Aib_3^- + 2OH^- \quad (4)$$

$(CN)_4^{2-}$ has a molar absorptivity of 4630 M^{-1} cm^{-1} at 285 nm.[23] The other reactants and products have no appreciable absorbance at this wavelength.

Results

Acid Dissociation Kinetics. The acid dissociation of $Ni^{II}(H_{-2}Aib_3)^-$ was investigated from –log [H$^+$] values of 0.30–5.69 in the presence and absence of buffers (see Table I and Figure 1). The reactions had small contributions from general-acid catalysis. The dependence of the dissociation rate on the concentration of buffers was measured at various [H$^+$], and the values of k°_{obsd} are reported, where k°_{obsd} is defined by eq 5. The

$$k^\circ_{obsd} = k_{obsd} - k_{HB}[HB] \quad (5)$$

general-acid-catalyzed term (k_{HB}[HB]) was typically less than 5% of the observed rate constant. Also included in Table I are rate constants obtained from the initial rate data at –log [H$^+$] = 6.7–7.7. These values are not corrected for buffer contribution, which should be quite small at the low buffer concentration used in these reactions.

The plot of log k°_{obsd} vs. –log [H$^+$] (Figure 1) has a large linear region of slope –1 from –log [H$^+$] = 5.9–2.9. However, from –log [H$^+$] = 2.7–1.3 the slope becomes more positive and reaches a value of –0.5, before it becomes more negative again at lower –log [H$^+$] values. These deviations from a simple first-order dependence in [H$^+$] can be seen more readily in a plot of k°_{obsd} vs. [H$^+$] shown in Figure 2. The data indicate the formation of significant concentrations of an intermediate protonated species, which we designate as $Ni^{II}(H_{-2}Aib_3)H$.

The acid dissociation was followed with a vidicon–stopped-flow spectrophotometer,[22] which permitted a series of spectra to be

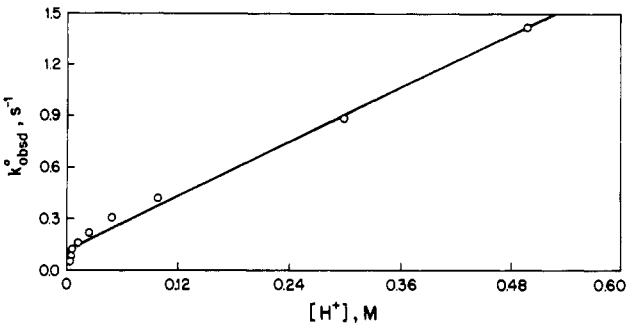

Figure 2. Hydrogen ion dependence of the reaction of $Ni^{II}(H_{-2}Aib_3)^-$ with acid at the highest acid concentrations studied. The solid line is the least-squares best fit to the data.

collected in rapid succession. At high-[acid] conditions, where a protonated intermediate is indicated from the hydrogen ion dependence, a rapid (<5 ms) spectral shift occurs in the d–d band of the complex, from the characteristic peak at 415 nm to one at 435 nm. This shift is followed by a time-dependent decrease in absorbance, in agreement with the k°_{obsd} values under these conditions.

These results are consistent with the rapid formation of $Ni^{II}(H_{-2}Aib_3)H$, where the proton has added to either a peptide oxygen or a carboxylate oxygen, as opposed to the peptide nitrogen. In previous studies,[24-26] this species has been termed an "outside-protonated" species to distinguish it from the much slower process, in which a metal–N(peptide) bond is broken to give the "inside-protonated" species, i.e. $Ni^{II}(H_{-1}Aib_3)$. The small spectral shift that is observed to a lower energy d–d band is expected because peptide oxygen protonation will remove some electron density from the peptide linkage. Hence, this protonation will weaken the metal–N(peptide) bond. In contrast, if an inside protonation occurred, the resulting nickel(II) complex would no longer be expected to be low spin but would be an octahedral, high-spin complex with no absorption band in the vicinity of 415–435 nm. Billo and co-workers[27] have shown that at least two deprotonated-peptide nitrogens must be coordinated for nickel(II) to maintain a square-planar geometry.

Thus, the designation of the protonated intermediate as an outside-protonated species is consistent with its rapid formation, its small spectral shift, the pH region in which it is seen, and the behavior of many other metal–peptide complexes.

The mechanism proposed to account for the observed hydrogen ion dependence, given in eq 6–9, is similar to that found for the

$$Ni^{II}(H_{-2}Aib_3)^- \xrightarrow{k_{0d}} \text{products} \quad (6)$$

$$Ni^{II}(H_{-2}Aib_3)^- + H^+ \underset{}{\overset{K_{1H}}{\rightleftharpoons}} Ni^{II}(H_{-2}Aib_3)H \quad (7)$$

$$Ni^{II}(H_{-2}Aib_3)H \xrightarrow{k_{1d}} \text{products} \quad (8)$$

$$Ni^{II}(H_{-2}Aib_3)H + H^+ \xrightarrow{k_2} \text{products} \quad (9)$$

triglycine complex.[26] The observed pseudo-first-order rate constant for this mechanism is given by eq 10.

$$k^\circ_{obsd} = \frac{k_{0d} + K_{1H}[H^+](k_{1d} + k_2[H^+])}{1 + K_{1H}[H^+]} \quad (10)$$

The equilibria and rate constants were resolved by a nonlinear least-squares computer program,[28] with the values of k°_{obsd} from

(22) Ridder, G. M.; Margerum, D. W. *Anal. Chem.* **1977**, *49*, 2098.
(23) Kolski, G. B.; Margerum, D. W. *Inorg. Chem.* **1968**, *7*, 2239.
(24) Barnet, M. T.; Freeman, H. C.; Buckingham, D. A.; van der Helm, D. *J. Chem. Soc., Chem. Commun.* **1970**, 367.
(25) Paniago, E. B.; Margerum, D. W. *J. Am. Chem. Soc.* **1972**, *94*, 6704.
(26) Bannister, C. E.; Margerum, D. W. *Inorg. Chem.* **1981**, *20*, 3149.
(27) Dorigatti, T. F.; Billo, E. J. *J. Inorg. Nucl. Chem.* **1980**, *37*, 1515.
(28) Nie, N.; Bent, D. H.; Hull, C. H. "Statistical Package for the Social Sciences"; McGraw-Hill: New York, 1970.

Table II. Protonation Constants and Dissociation Rate Constants for Nickel(II)–Peptide and Copper(II)–Peptide Complexes

const	Ni^{II}-$(H_{-2}Aib_3)^-$ [a]	Ni^{II}-$(H_{-2}G_3)^-$	Cu^{II}-$(H_{-2}Aib_3)^-$ [d]	Cu^{II}-$(H_{-2}G_3)^-$ [e]
k_{0d}, s^{-1}	$<10^{-7}$	0.05 [b]		0.12
K_{1H}, M^{-1}	$10^{2.1}$	$<10^{2.2}$ [c]		
k_{1d}, s^{-1}	2.2×10^{-1}			
$k_{1d}K_{1H}$, $M^{-1}\ s^{-1}$	2.8×10^{1}	9.5×10^{4} [c]	1.9×10^{6}	4.9×10^{6}
k_2, $M^{-1}\ s^{-1}$	2.4			
$K_{1H}k_2$, $M^{-2}\ s^{-1}$	2.8×10^{2}	1.1×10^{8} [c]		

[a] μ = 1.0 ($NaClO_4$), 25.0 (1) °C; this work. [b] μ = 0.16 ($NaClO_4$), 25.0 (1) °C; ref 32. [c] μ = 0.30 ($NaClO_4$), 25.0 (1) °C; ref 26. [d] μ = 0.10 ($NaNO_3$), 25.0 (1) °C; ref 18. [e] μ = 0.10 ($NaClO_4$), 25.0 (1) °C; ref 19.

Table III. Values of the Stability Constant for $Ni^{II}(H_{-2}Aib_3)^-$ [a]

−log [H^+]	% completion	log β_{1-21}	−log [H^+]	% completion	log β_{1-21}
6.95	97.0	−9.62	7.24	86.7	−9.69
6.96	96.0	−9.51	7.31	78.6	−9.60
7.04	94.7	−9.59	7.31	80.9	−9.68
7.04	94.8	−9.58	7.42	77.2	−9.73
7.15	90.9	−9.63	7.43	70.8	−9.72
7.14	92.4	−9.69	7.54	61.1	−9.76
7.24	86.3	−9.67			−9.65 (7) (av)

[a] $[Ni]_{tot} = 2.54 \times 10^{-5}$ M, $[PO_4]_{tot} = 2 \times 10^{-3}$ M, μ = 0.1 ($NaClO_4$), A_{init} (10-cm cell) = 1.589, 25 ± 1 °C, 250 nm.

−log [H^+] = 0.30–5.69. Under these conditions the buffer contributions have been subtracted, and the reactions are not reversible. The resolved values of the individual constants are given in Table II, along with the corresponding values for similar complexes. From these values it can be seen that the direct dissociation pathway, k_{0d}, is not a significant one for Ni^{II}-$(H_{-2}Aib_3)^-$. This is consistent with the fact that the plot of log k°_{obsd} in Figure 1 shows no tendency to level off even at −log [H^+] values of 7.7. The initial rate data from −log [H^+] values of 6.7–7.7 fall along the predicted k°_{obsd} values.

Acid Dissociation Equilibrium. The dissociation of Ni^{II}-$(H_{-2}Aib_3)^-$ was carried out from −log [H^+] = 6.7–7.7, under conditions where the reaction did not go to completion. In these experiments, the equilibrium position ranged from 97% to 61% completion. The equilibrium position was taken as the point where the absorbance showed no change for 3 or more days. The times required to reach equilibrium (16–26 days) were in good agreement with the times calculated from the dissociation rate constant determined above, under the reversible conditions of the experiments. The measurement of this equilibrium condition allows the calculation of the overall stability constant for the Ni^{II}-$(H_{-2}Aib_3)^-$ complex, β_{1-21}, as defined in eq 1. Table III shows the values of log β_{1-21} and the percent completion at the equilibrium condition, for the various values of −log [H^+] investigated. All values of β_{1-21} reported are corrected for the formation of $Ni(HPO_4)$ (log β_{111} = 2.1),[29] the pK of $H_2PO_4^-$ (pK = 6.73),[30] and the pK_{NH} of Aib_3 (pK_{NH} = 8.11).[9] Under the conditions used, the values of K_{sp} for $Ni_3(PO_4)_2$ and $Ni(OH)_2$ were not exceeded. The values of β_{1-21} do not show a significant trend with −log [H^+], and the average value of log β_{1-21} is −9.65 (7).

Cyanide Reactions. The reaction of $Ni^{II}(H_{-2}Aib_3)^-$ with excess cyanide ion was also investigated. All reactions were run at −log[H^+] = 10.20, were buffered with borate (0.02 M), μ = 0.1 ($NaClO_4$), and were run at 25.0 (1) °C. The reactions were first order in the nickel complex; Table IV gives the values of k_{obsd} for the range of [CN^-] investigated. A plot of k_{obsd} vs. [CN^-]^2 (Figure 3) is linear, with a slope of 13.19 (2) $M^{-2}\ s^{-1}$ and an intercept of 2.0 (1) $\times 10^{-4}\ s^{-1}$. As seen in Figure 3, the reaction is second order in [CN^-], under the conditions investigated, with a small contribution from a [CN^-]-independent term. The mechanism proposed to explain this dependence is given in eq 11–14.

Table IV. Observed Rate Constants for the Reaction of $Ni^{II}(H_{-2}Aib_3)^-$ with Cyanide [a]

[CN^-], [b] M	10^3k_{obsd}, s^{-1}	[CN^-], [b] M	10^3k_{obsd}, s^{-1}
0.0072	0.86 (3)	0.0144	2.94 (1)
0.0090	1.28 (1)	0.0180	4.44 (2)
0.0108	1.76 (1)	0.0360	17.3 (2)

[a] $[Ni]_{tot} = 5 \times 10^{-5}$ M, $[B]_{tot}$ = 0.02 M, μ = 0.1 ($NaClO_4$), −log [H^+] = 10.20, 25.0 (1) °C, 285 nm, 2-cm cell. [b] [CN^-] is corrected for the pK_a of HCN, which is 9.01 at 25 °C, μ = 0.1.[31]

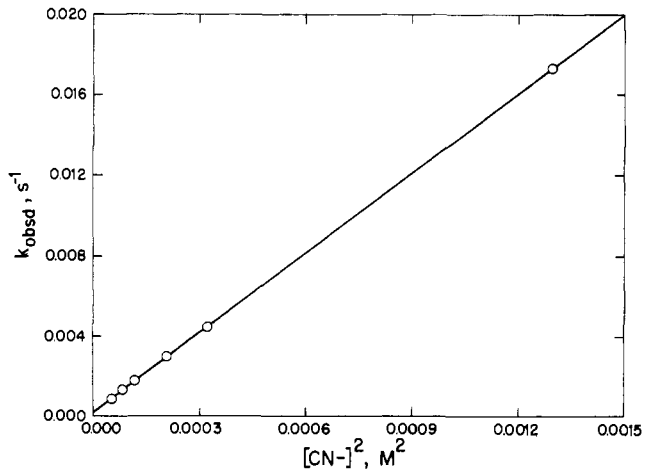

Figure 3. Dependence of the observed rate constant on [CN^-]^2 for the reaction of $Ni^{II}(H_{-2}Aib_3)^-$ with cyanide ion at −log [H^+] = 10.20 (0.02 M $[BO_3^{3-}]_{tot}$), μ = 0.1 ($NaClO_4$), and 25.0 (1) °C. The solid line is the least-squares best fit to the data.

$$Ni^{II}(H_{-2}Aib_3)^- + CN^- \underset{K_1}{\overset{fast}{\rightleftharpoons}} Ni^{II}(H_{-2}Aib_3)(CN)^{2-} \quad (11)$$

$$Ni^{II}(H_{-2}Aib_3)(CN)^{2-} \xrightarrow{k_{1d}} \text{products} \quad (12)$$

$$Ni^{II}(H_{-2}Aib_3)(CN)^{2-} + CN^- \underset{k_{-2}}{\overset{k_2}{\rightleftharpoons}} Ni^{II}(H_{-2}Aib_3)(CN)_2^{3-} \quad (13)$$

$$Ni^{II}(H_{-2}Aib_3)(CN)_2^{3-} + CN^- \xrightarrow{k_3} \text{products} \quad (14)$$

The fast preequilibrium in eq 11 is the formation of an intermediate mixed-ligand complex. The formation of this complex results in a rapid (k_{obsd} > 300 s^{-1}) decrease in absorptivity of the $Ni^{II}(H_{-2}Aib_3)^-$ d–d band at 415 nm. The formation of this intermediate can be seen by the difference between the spectrum of a mixture of $Ni^{II}(H_{-2}Aib_3)^-$ and CN^- and the spectrum of a solution containing only $Ni^{II}(H_{-2}Aib_3)^-$. The spectra show a rapid decrease in molar absorptivity of the band at 415 nm, followed by a slower conversion to the product, $Ni(CN)_4^{2-}$. The magnitude of the initial absorbance decrease at 415 nm does not change when the [CN^-] is increased from 1×10^{-3} M to 2×10^{-3} M. This shows that the intermediate is >90% formed when the cyanide ion concentration is 10^{-3} M, so the association constant, K_1, is greater than $10^4\ M^{-1}$.

The small intercept of the plot of k_{obsd} vs. [CN^-]^2 (Figure 3) is indicative of the water-assisted dissociation of the intermediate mixed-ligand complex ($k_{1d} = 2 \times 10^{-4}\ s^{-1}$), shown in eq 12. No appreciable concentration of the second proposed mixed-ligand complex, $Ni^{II}(H_{-2}Aib_3)(CN)_2^{3-}$, is observed. A steady-state approximation can, therefore, be applied to this species. This yields the rate expressions given in eq 15–17. Since $K_1[CN^-] >> 1$,

(29) Taylor, R. S.; Diebler, H. *Bioinorg. Chem.* **1976**, *6*, 247.
(30) Martell, A. E.; Smith, R. M. "Critical Stability Constants" Plenum Press: New York, 1974; Vol. 1.
(31) Tsonopoulos, C.; Coulson, D. M.; Inman, L. B. *J. Chem. Eng. Data* **1976**, *21*, 190.
(32) Billo, E. J.; Margerum, D. W. *J. Am. Chem. Soc.* **1970**, *92*, 6811.
(33) Bossu, F. P.; Margerum, D. W. *Inorg. Chem.* **1977**, *16*, 1210.

$$\text{rate} = -d[Ni^{II}(H_{-2}Aib_3)]_{tot}/dt = k_{obsd}[Ni^{II}(H_{-2}Aib_3)]_{tot} \quad (15)$$

$$[Ni^{II}(H_{-2}Aib_3)]_{tot} = [Ni^{II}(H_{-2}Aib_3)^-] + [Ni^{II}(H_{-2}Aib_3)(CN)^{2-}] \quad (16)$$

$$k_{obsd} = \frac{k_2k_3K_1[CN^-]^3}{(k_{-2} + k_3[CN^-])(1 + K_1[CN^-])} + \frac{k_{1d}K_1[CN^-]}{1 + K_1[CN^-]} \quad (17)$$

eq 17 simplifies to eq 18. A plot of $[CN^-]/(k_{obsd} - k_{1d})$ vs.

$$k_{obsd} = \frac{k_2k_3[CN^-]^2}{k_{-2} + k_3[CN^-]} + k_{1d} \quad (18)$$

$1/[CN^-]$ (Figure 4) is linear, with slope = $k_{-2}/(k_2k_3)$ = 0.078 (2) and a negligible intercept. Since the intercept is negligible, the condition of $k_{-2} >> k_3[CN^-]$ is satisfied. Equation 18 can then be simplified to eq 19, which gives the observed second-order

$$k_{obsd} = (k_2k_3/k_{-2})[CN^-]^2 + k_{1d} \quad (19)$$

dependence on $[CN^-]$. The value of the third-order rate constant obtained from this plot (k_2k_3/k_{-2}) is in good agreement with that obtained from the plot of k_{obsd} vs. $[CN^-]^2$, and the average value for the third-order rate constant is 13.0 (2) $M^{-2}s^{-1}$.

Discussion

The acid dissociation rate constant ($K_{1H}k_{1d}$ = 28 M^{-1} s^{-1}) and the β_{1-21} value can be used to calculate a formation rate constant (k_f = 6.3 × 10^{-9} s^{-1}) that corresponds to the rate expression $d[Ni(H_{-2}Aib_3)^-]/dt = k_f[Ni^{2+}][Aib_3^-]/[H^+]$. With a p$K_a$ value[9] of 8.11 for $HAib_3^{\pm}$, this expression predicts a first half-life of 62 h for 10^{-3} M reactants at pH 7. At pH 8.1 the first half-life is 0.88 h, and at higher pH the solubility of $Ni(OH)_2$ is exceeded. These calculations are consistent with the sluggish rate of formation that was observed.

Table II compares the resolved rate constants for the protonation and dissociation of the nickel(II) and copper(II) complexes of Aib_3 and G_3. A second-order proton-transfer rate constant ($k_{1d}K_{1H}$) has been determined for all four complexes. The copper(II)–peptide complexes are more basic and have much larger proton-transfer rate constants than the nickel(II)–peptide complexes. The change from G_3 to Aib_3 decreases the rate constants by only a factor of 2.6 for the copper(II) complexes. On the other hand, the corresponding ligand change decreases the proton-transfer rate constant by a factor of 3400 for the nickel(II) complexes. It is clear that the change is not due merely to steric effects of the methyl groups. Otherwise the results would be the same for both copper and nickel complexes.

It is possible to resolve several constants (k_{1d}, K_{1H}, and k_2) for the $Ni^{II}(H_{-2}Aib_3)^-$ reactions that could not be resolved for the $Ni^{II}(H_{-2}G_3)^-$ complex because the latter reactions were too rapid. Thus, appreciable concentrations of the outside-protonated species, $Ni^{II}(H_{-2}Aib_3)H$, were detected, and its K_{1H} value of $10^{2.1}$ agrees with the upper limit of $10^{2.2}$ set for $Ni^{II}(H_{-2}G_3)H$. The third-order protonation rate constant ($K_{1H}k_2$) is a factor of 4 × 10^5 smaller for the nickel(II) complex of Aib_3 than for the G_3 complex. Similarly, the water dissociation rate constant, k_{0d}, is at least 5 × 10^5 smaller for the Aib_3 complex. Hence, with nickel(II), all three dissociation rate paths (k_{0d}, $K_{1H}k_{1d}$, and $K_{1H}k_2$) are markedly slower for the Aib_3 complex.

The overall stability constants (β_{1-21}) for the G_3 and Aib_3 complexes of copper(II) and nickel(II) are compared in Table V. The copper(II) complexes are much more stable, but the ratio of Aib_3/G_3 stability constants is only 63. For nickel(II), the Aib_3 complex is 1500 times more stable than the G_3 complex, which parallels the factor of 3400 seen in the diminished-acid dissociation rate constant.

The six methyl groups on the backbone of the Aib_3 ligand have an electron-donating effect that gives rise to a substantially increased donor strength of the peptide nitrogens. The magnitude of this effect is not very obvious in the pK_a values of $H_2Aib_3^+$ and $HAib_3^{\pm}$, which are only 0.62 and 0.22 log unit larger, respectively, than the pK_a values of $H_2G_3^+$ and $HG_3^{\pm}$. However, steric interference in the aquation of the ions probably serves to diminish the effect of the methyl groups on the observed basicity of the amino group.[9] The increased donor strength of Aib_3 can explain the factors of 63 and 1500 seen in the increased stability of the copper(II) and nickel(II) complexes. There is substantial additional evidence of this increase in donor strength from comparison of the X-ray crystal structures of the nickel(II) and copper(II) complexes of Aib_3[17] and similar glycyl complexes.[34,35] The metal–N(peptide) bond lengths are 0.03–0.04 Å shorter in the Aib_3 complexes of both metals, as compared to those in the glycyl peptide complexes. There is also spectral evidence to confirm the enhanced donor strength. Table VI contains the values of λ_{max} for a series of tripeptide complexes of copper(II) and nickel(II). The position of the d–d band shifts to lower wavelength as the progression from G_3 to A_3 (A = L-alanyl) to Aib_3 is followed. As the number of methyl groups increases, an increase in donor

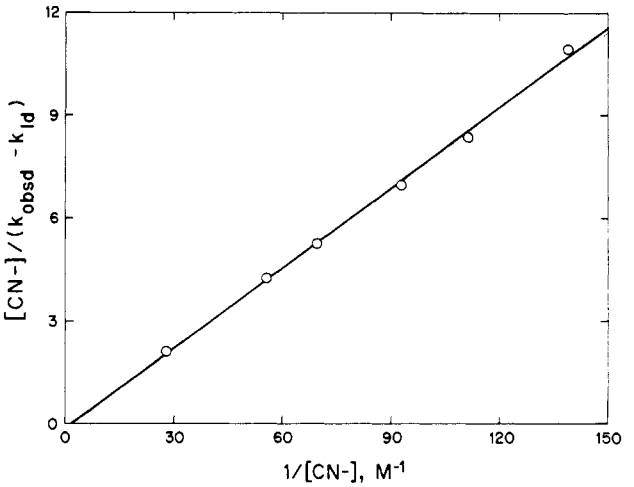

Figure 4. Dependence of $[CN^-]/(k_{obsd} - k_{1d})$ on $1/[CN^-]$ for the reaction of $Ni^{II}(H_{-2}Aib_3)^-$ with cyanide ion. The value of k_{1d} is obtained from the intercept of Figure 3. The solid line is the least-squares best fit to the data.

Table V. Overall Stability Constants (β_{1-21}) and M(III,II) Reduction Potentials for Nickel–Peptide and Copper–Peptide Complexes[a]

complex	log β_{1-21}	E^0, V vs. NHE
$Ni^{II}(H_{-2}Aib_3)^-$	−9.65[b]	0.82[c]
$Ni^{II}(H_{-2}G_3)^-$	−12.82[d]	0.85[e]
$Cu^{II}(H_{-2}Aib_3)^-$	−4.95[f]	0.66[g]
$Cu^{II}(H_{-2}G_3)^-$	−6.75[h]	0.92[i]

[a] μ = 0.1 ($NaClO_4$), 25.0 (1) °C. [b] This work. [c] Reference 16. [d] μ = 0.16 ($NaClO_4$); ref 32. [e] Reference 33. [f] Reference 9. [g] Reference 6. [h] Reference 30. [i] Reference 34.

Table VI. Absorption Maxima of d–d Bands for $M(H_{-2}L)^-$ Complexes

L	λ_{max}, nm	
	Ni^{II}	Cu^{II}
G_3	430[a]	553[b]
A_3	426[a]	544[b]
Aib_3	415[c]	508[b]

[a] Reference 33. [b] Reference 38. [c] This work.

(34) Bossu, F. P.; Chellappa, K. L.; Margerum, D. W. *J. Am. Chem. Soc.* **1977**, *99*, 2195.
(35) Margerum, D. W.; Dukes, G. R. "Metal Ions in Biological Systems"; Sigel, H., Ed.; Marcel Dekker: New York, 1974; Vol. I.
(36) Freeman, H. C.; Guss, J. M.; Sinclair, R. L. *Acta Crystallogr., Sect B: Struct. Crystallogr. Cryst. Chem.* **1978**, *B34*, 2459; *J. Chem. Soc., Chem. Commun.* **1968**, 485.
(37) Freeman, H. C.; Taylor, M. R. *Acta Crystallogr.* **1965**, *18*, 939.
(38) Hamburg, A. W. Ph.D. Dissertation, Purdue University, West Lafayette, IN, 1982.
(39) Pagenkopf, G. K.; Brice, V. T. *Inorg. Chem.* **1975**, *14*, 3118.
(40) Pagenkopf, G. K. *Inorg. Chem.* **1974**, *13*, 1591.

Table VII. Resolved Rate Constants for the Reaction of $Ni^{II}(H_{-2}L)^-$ with Cyanide Ion

const	L = G_3^- [a]	L = Aib_3^-
K_1, M^{-1}	$>10^5$	$>10^4$
k_{1d}, s^{-1}		2.0×10^{-4}
k_2, $M^{-1}\ s^{-1}$	5.9	
k_2k_3/k_{-2}, $M^{-2}\ s^{-1}$	1.3×10^3	1.3×10^1
K_2, M^{-1}	17	not obsd [b]

[a] References 39 and 40. [b] This is not observed even though $[CN^-]$ is a factor of 1.5–36 higher than in the G_3 study.

strength occurs, which results in the shift of the d–d band to higher energy.

The crystal field stabilization energy (CFSE) for the square-planar d^8 nickel(II) complex should be greater than that for the d^9 copper(II) complex. This is reflected in shorter bonds for the nickel complex. Recent crystal structures[17] show that the average equatorial bond lengths are 1.83 Å for $Ni^{II}(H_{-2}Aib_3)^-$ compared to 1.92 Å for $Cu^{II}(H_{-2}Aib_3)^-$. The stability constant for the copper(II) complex is larger because electron-pairing energy is required to form the low-spin square-planar nickel(II) complex. The d^8 nickel(II) system shows a greater increase in stability constant for the Aib_3, relative to the G_3 complex, as compared to d^9 copper(II) system. This can be attributed to the larger gain in CFSE for the nickel(II) system as the donor strength of the ligand increases.

The nickel(III,II) and copper(III,II) reduction potentials have been measured for the complexes of Aib_3[6,16] and G_3.[33,34] The ratios of the stabilities of the complexes of divalent nickel and copper with Aib_3 and G_3 are now known. This information can be used to calculate the ratios (R, eq 20–22) of the stabilities of the

$$M^{II} + G_3^- \underset{-2H^+}{\overset{\beta_{1-21}}{\rightleftharpoons}} M^{II}(H_{-2}G_3)^- \overset{-e^-}{\underset{E^0}{\rightleftharpoons}} M^{III}(H_{-2}G_3) \quad (20)$$

$$M^{II} + Aib_3^- \underset{-2H^+}{\overset{\beta_{1-21}}{\rightleftharpoons}} M^{II}(H_{-2}Aib_3)^- \overset{-e^-}{\underset{E^0}{\rightleftharpoons}} M^{III}(H_{-2}Aib_3) \quad (21)$$

$$R = \frac{[M(H_{-2}Aib_3)][G_3^-]}{[M(H_{-2}G_3)][Aib_3^-]} \quad (22)$$

trivalent metal complexes of these two ligands. The R values follow the sequence Cu^{II} ($10^{1.8}$) < Ni^{II} ($10^{3.2}$) ≤ Ni^{III} ($10^{3.7}$) << Cu^{III} ($10^{6.2}$). In other words, $Ni^{III}(H_{-2}Aib_3)$ is over 5000 times more stable than $Ni^{III}(H_{-2}G_3)$, and $Cu^{III}(H_{-2}Aib_3)$ is almost 1.6 million times more stable than $Cu^{III}(H_{-2}G_3)$. Thus, the inductive effect of the six methyl groups on the copper(III) complex is enormous. The enhanced stability is consistent with previous observations of the increased thermal stability of the nickel(III) and copper(III) complexes of Aib_3, relative to that of the corresponding complexes of G_3,[6] and the large CFSE, which is expected for a d^8 trivalent metal ion with a square-planar geometry.[32]

The reaction of $Ni^{II}(H_{-2}Aib_3)^-$ with cyanide ion is also markedly slower than the corresponding reaction of $Ni^{II}(H_{-2}G_3)^-$. The values of the resolved rate constants for the reactions of both of these complexes with cyanide ion are given in Table VII. These complexes both rapidly form stable 1:1, cyanide ion mixed-ligand intermediates. The complexes react by a similar mechanism, with a rate step that depends on $[CN^-]^2$, which carries the major portion of the reaction. The third-order rate constant for this process, k_2k_3/k_{-2}, as defined in eq 19, is ~100 times smaller for the Aib_3 complex than the corresponding value for $Ni^{II}(H_{-2}G_3)^-$. In the case of the G_3 complex, there is kinetic evidence for the formation of significant concentrations of a second intermediate, $Ni^{II}(H_{-2}G_3)(CN^-)_2^{3-}$. In the present study, there is no evidence for the formation of such a species, despite the use of cyanide concentrations up to 36 times that used in the G_3 study. The failure to observe a second intermediate is presumably due to the more rigid steric restraints. The methyl groups on the Aib_3 peptide backbone limit the flexibility of the ligand, to the extent that the formation of the second mixed-ligand species is unfavorable.

The 1:1 mixed-ligand intermediate is probably an equatorial cyanide adduct, where cyanide replaces the carboxylate oxygen in the coordination sphere of the nickel atom. The main evidence in favor of an equatorial adduct, as opposed to an axial adduct, is the magnitude of the association constant (K_1 as defined in eq 11). Studies on axial adducts of nickel(III)–peptide complexes[14] give association constants that are all smaller than that obtained for K_1 in this study. It is expected that the nickel(II) complexes would have smaller axial association constants than the nickel(III) complexes, due to the smaller charge of nickel(II) and its preference for square-planar geometries. The rate of the opening of the carboxylate chelate ring has been estimated as less than 50 s^{-1} for $Cu^{II}(H_{-2}Aib_3)^-$.[18] The rate of formation of the $Ni^{II}(H_{-2}Aib_3)(CN)^{2-}$ intermediate is significantly faster than this, which suggests that the observed process is the cyanide-assisted displacement of the carboxylate oxygen from the nickel.

In general, all of the observed reactions of $Ni^{II}(H_{-2}Aib_3)^-$ except electron transfer are significantly slower than the corresponding reactions of $Ni^{II}(H_{-2}G_3)^-$. The slowness of the reactions is a reflection of the enhanced stability of the Aib_3 complex, as compared to that of the G_3 complex. The electron-donating effect of the methyl groups on the Aib_3 backbone give rise to increased donor strength of the peptide nitrogens, which is effective in stabilizing the complexes. The stabilizing effect is even greater for the trivalent metal complexes than for the divalent metal complexes of copper and nickel.

Acknowledgment. This work was supported by Public Health Service Grant No. GM-12152 from the National Institute of Medical Sciences.

Registry No. CN^-, 57-12-5.

Contribution from the Department of Chemistry, Washington University, St. Louis, Missouri 63130

Electron Self-Exchange in Bis(imidazole)iron Porphyrins

ATAOLLAH SHIRAZI, MICHAEL BARBUSH, SUCHITRA GHOSH, and DABNEY WHITE DIXON*

Received November 26, 1984

Self-exchange rate constants have been measured for a series of bis(imidazole)iron porphyrins. The rate constants in CD_2Cl_2 at −21 °C for bis(1-methylimidazole)-ligated tetraphenylporphyrins are as follows ($M^{-1}\ s^{-1}$): tetraphenylporphyrin (TPP), 8.1×10^7; 3-MeTPP, 5.3×10^7; 4-MeTPP, 9.7×10^7; 4-OMeTPP, 6.8×10^7; 2,4,6-Me_3TPP, 1.6×10^8. Increasing the steric bulk either at the heme edge or on the axial imidazole has little effect on the rate constant for electron self-exchange. However, complexes with axial imidazoles bearing an N–H substituent have self-exchange rate constants that are a factor of 2–3 smaller than those with *N*-alkyl substituents. The rate constants measured in this study are only slightly larger than those observed for short cytochromes. ^1H NMR spectral assignments of the $Fe^{II}TPP(RIm)_2$ complexes are reported.

Heme proteins are ubiquitous electron-transfer agents in biological processes. The role of the protein in controlling the rate or specificity of electron transfer is currently the subject of intense study.[1-9] A variety of factors have been postulated to be im-

0020-1669/85/1324-2495$01.50/0